Suppression of Nonlinear Interactions in Resonant Macroscopic Quantum Devices : the Example of the Solid-State Ring Laser Gyroscope

Sylvain Schwartz, François Gutty, Gilles Feugnet, Philippe Bouyer, Jean-Paul Pocholle

HAL Id: hal-00202466
https://hal.science/hal-00202466

Submitted on 7 Jan 2008

Suppression of Nonlinear Interactions in Resonant Macroscopic Quantum Devices : the Example of the Solid-State Ring Laser Gyroscope

Sylvain Schwartz[1], François Gutty[2], Gilles Feugnet[1], Philippe Bouyer[3] and Jean-Paul Pocholle[1]

[1] *Thales Research and Technology France, Route Départementale 128, F-91767 Palaiseau Cedex, France*
[2] *Thales Avionics, 40 rue de la Brelandière, BP 128, F-86101 Châtellerault, France*
[3] *Laboratoire Charles Fabry de l'Institut d'Optique, CNRS and Université Paris-Sud, Campus Polytechnique, RD 128, F-91127 Palaiseau Cedex, France*[*]

(Dated: 7th January 2008)

We study the suppression of nonlinear interactions in resonant macroscopic quantum devices in the case of the solid-state ring laser gyroscope. These nonlinear interactions are tuned by vibrating the gain medium along the cavity axis. Beat note occurrence under rotation provides a precise measurement of the strength of nonlinear interactions, which turn out to vanish for some discrete values of the amplitude of vibration. Our theoretical description, in very good agreement with the measured data, suggests the use of a higher vibration frequency to achieve quasi-ideal rotation sensing over a broad range of rotation speeds. We finally underline the analogy between this device and some other macroscopic quantum rotation sensors, such as ring-shaped superfluid configurations, where nonlinear interactions could be tuned for example by the use of magnetically-induced Feschbach resonance.

The use of macroscopic quantum effects for rotation sensing in ring-shaped configurations has been extensively studied in the case of both optical systems [1, 2, 3] and superfluids [4, 5], either liquid helium [6, 7] or Bose-Einstein condensed gases [8, 9, 10, 11, 12]. As pointed out in [13, 14], nonlinear interactions play a crucial role in the dynamics of such devices, as they can hinder or affect their ability to sense rotation, even when counteracted by other coupling sources. Consequently, the possibility of tuning or even suppressing nonlinear interactions is of great importance for using these devices as rotation sensors.

Several systems offer the possibility of controlling the strength of their nonlinearities. For example, in the case of gas ring laser gyroscopes, one can considerably lower mode competition by tuning the cavity out of resonance with the atoms at rest, resulting in the quasi-suppression of nonlinear interactions [1]. In the case of atomic systems, it is also possible to tune and even suppress nonlinear interactions, by using Feshbach resonance [15, 16, 17]. As regards solid-state ring lasers, we have recently demonstrated [14] the possibility of stable rotation sensing thanks to the circumvention of mode competition by the use of an additional stabilizing coupling. However, nonlinear interactions are still present in this configuration, and can even be quantitatively observed [14, 18].

In this Letter, we report the experimental and theoretical study of a novel technique intended to tune and suppress nonlinear interactions in a solid-state ring laser gyroscope, similarly to the case of scattering length control in an atomic system. This is achieved by vibrating the gain crystal along the optical axis of the laser cavity, considering the fact that nonlinear interactions in a solid-state ring laser result mainly from mutual coupling between the counterpropagating modes induced by the population inversion grating established in the amplifying medium [3, 14]. Using the quantitative information on the strength of the nonlinear interactions provided by the beat note between the counterpropagating laser beams [14], we demonstrate experimentally the possibility of suppressing these interactions for some discrete values of the amplitude of the crystal movement. We eventually derive, in the limit of high vibration frequencies, a very simple condition for rotation sensing and point out the similarity with the equivalent condition for a toroidal Bose-Einstein condensed gas, resulting from the toy model of [13] where the effects of scattering length tuning described in [15] are included.

The solid-state ring laser gyroscope can be described semiclassically, assuming one single identical mode in each direction of propagation (something which is guaranteed by the attenuation of spatial hole burning effects thanks to the gain crystal movement [19]), one single identical state of polarization and plane wave approximation. The electrical field inside the cavity can then be written as follows :

$$E(x,t) = \mathrm{Re}\left\{ \sum_{p=1}^{2} \tilde{E}_p(t) e^{i(\omega_c t + \mu_p kx)} \right\} ,$$

where $\mu_p = (-1)^p$ and where ω_c and k are respectively the angular and spatial average frequencies of the laser, whose longitudinal axe is associated with the x coordinate. In the absence of crystal vibration, the equations of evolution for the slowly-varying amplitudes $\tilde{E}_{1,2}$ and for the population inversion density N have the following

expression [3, 14] :

$$\frac{\mathrm{d}\tilde{E}_{1,2}}{\mathrm{d}t} = -\frac{\gamma_{1,2}}{2}\tilde{E}_{1,2} + i\frac{\tilde{m}_{1,2}}{2}\tilde{E}_{2,1} + i\mu_{1,2}\frac{\Omega}{2}\tilde{E}_{1,2}$$
$$+\frac{\sigma}{2T}\left(\tilde{E}_{1,2}\int_0^L N\mathrm{d}x + \tilde{E}_{2,1}\int_0^L Ne^{-2i\mu_{1,2}kx}\mathrm{d}x\right)$$

$$\frac{\partial N}{\partial t} = W_{\mathrm{th}}(1+\eta) - \frac{N}{T_1} - \frac{aNE(x,t)^2}{T_1} ,$$

where $\gamma_{1,2}$ are the intensity losses per time unit for mode, $\tilde{m}_{1,2}$ are the backscattering coefficients, Ω difference between the eigenfrequencies of the co propagating modes (including the effect of rotatio further), σ is the laser cross section, T is the round-trip time, η is the relative excess of pumping above the threshold value W_{th}, T_1 is the lifetime population inversion and a is the saturation paran Throughout this paper we shall neglect dispersion e considering the fact that the Nd-YAG gain width is larger than the laser cavity free spectral range. backscattering coefficients, which depend on spati homogeneities of the propagation medium [20], ha following expression [18] :

$$\tilde{m}_{1,2} = -\frac{\omega_c}{\bar{\varepsilon}cT}\oint_0^L\left[\varepsilon(x) - \frac{i\kappa(x)}{\omega_c}\right]e^{-2i\mu_{1,2}kx}\mathrm{d}x ,$$

where $\varepsilon(x)$ and $\kappa(x)$ are respectively the dielectri stant and the fictitious conductivity along the perimeter in the framework of an ohmic losses [21], where c is the speed of light in vacuum and w stands for the spatial average of ε. In order to coun mode competition effects and ensure beat regime o tion under rotation, an additional stabilizing coupling as described in [14] is introduced, resulting in losses of the following form :

$$\gamma_{1,2} = \gamma - \mu_{1,2}Ka(|\tilde{E}_1|^2 - |\tilde{E}_2|^2) , \qquad (4)$$

where $\gamma = \bar{\kappa}/\bar{\varepsilon}$ is the average loss coefficient and where $K > 0$ represents the strength of the stabilizing coupling.

We assume the following sinusoidal law to account for the gain crystal vibration :

$$x_c(t) = \frac{x_m}{2}\sin(2\pi f_m t) , \qquad (5)$$

where $x_c(t)$ is the coordinate, in the frame of the laser cavity, of a given reference point attached to the crystal, and where x_m and f_m are respectively the amplitude and the frequency of the vibration movement. The population inversion density function in the frame of the vibrating crystal $N_c(x,t)$ is ruled by the following equation :

$$\frac{\partial N_c}{\partial t} = W_{\mathrm{th}}(1+\eta) - \frac{N_c}{T_1} - \frac{aN_cE(x+x_c(t),t)^2}{T_1} , \quad (6)$$
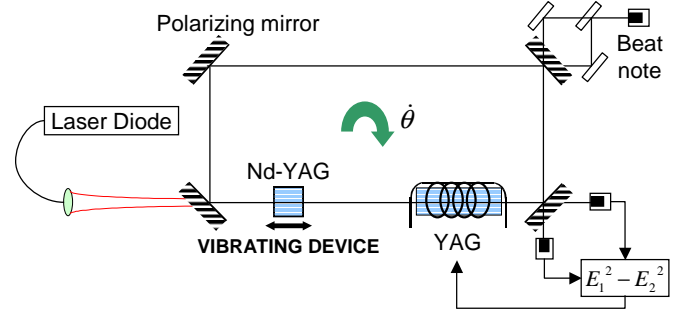

Figure 1: Scheme of our experimental setup. The diode-pumped vibrating Nd-YAG crystal is placed inside a 22-cm ring cavity on a turntable. Losses of the form (4) are created by a feedback loop acting on a Faraday rotator (an additional YAG crystal inside a solenoid), in combination with a polarizing mirror and a slight non-planarity of the cavity (not drawn here). Two photodiodes are used for generating the error signal of the feedback loop. A third photodiode measures the frequency of the beat note between the counterpropagating modes.

where $E(x,t)$ refers to the electric field in the cavity (non-vibrating) frame. Moreover, $N_c(x,t)$ can be deduced from its equivalent in the cavity frame $N(x,t)$ by the identity $N_c(x,t) = N(x+x_c(t),t)$, resulting in the following expressions :

$$\begin{cases} \int_0^L N(x,t)\mathrm{d}x = \int_0^L N_c(x,t)\mathrm{d}x , \\ \int_0^L N(x,t)e^{2ikx}\mathrm{d}x = e^{2ikx_c(t)}\int_0^L N_c(x,t)e^{2ikx}\mathrm{d}x . \end{cases}$$

The backscattering coefficients (3) acquire in the presence of the crystal vibration the following time-dependent form :

$$\tilde{m}_{1,2}(t) = \tilde{m}_{1,2}{}^c e^{-2i\mu_1,2kx_c(t)} + \tilde{m}_{1,2}{}^m , \qquad (7)$$

where $\tilde{m}_{1,2}{}^c$ and $\tilde{m}_{1,2}{}^m$, which are time-independent, account for the backscattering due respectively to the crystal at rest and to any other diffusion source inside the laser cavity (including the mirrors). As regards the difference Ω between the eigenfrequencies of the counterpropagating modes, it results from the combined effects of the rotation (Sagnac effect [22]) and of the crystal movement in the cavity frame (Fresnel-Fizeau drag effect [23]), resulting in the following expression :

$$\frac{\Omega}{2\pi} = \frac{4A}{\lambda L}\dot{\theta} - \frac{2\dot{x}_c(t)l(n^2-1)}{\lambda L} , \qquad (8)$$

where A is the area enclosed by the ring cavity, $\lambda = 2\pi c/\omega_c$ is the emission wavelength, $\dot{\theta}$ is the angular velocity of the cavity around its axis, and l and n are respectively the length and the refractive index of the crystal (dispersion terms are shown to be negligible in this case).

The dynamics of the solid-sta[...]
with a vibrating gain medium is [...]
framework of our theoretical descr[...]
equations :

$$\frac{\mathrm{d}\tilde{E}_{1,2}}{\mathrm{d}t} = -\frac{\gamma_{1,2}}{2}\tilde{E}_{1,2} + i\frac{\tilde{m}_{1,2}}{2}\tilde{E}_{2,1}$$

$$+\frac{\sigma}{2T}\left(\tilde{E}_{1,2}\int_0^L N_c\mathrm{d}x + \tilde{E}_{2,1}e^{2ikx_{}}\right.$$

where $\gamma_{1,2}$, x_c, N_c, $\tilde{m}_{1,2}$ and Ω [...]
tions (4), (5), (6), (7) and (8). [...]
analysis that the solid-state ring l[...]
tion sensor, from the crystal vibr[...]
and complementary ways :

- the contrast of the popula[...]
  which is responsible for no[...]
  duced on both conditions th[...]
  movement is of the same or[...]
  the step of the optical grati[...]
  of μm) and that the period[...]
  is significantly larger than t[...]
  response time T_1; the ato[...]
  longer confined into a nod[...]
  – see eq. (6) –, and becom[...]
  average value of the electric[...]
  dependent of their position[...]
  when the laser is not rotati[...]
  tion $J_0(kx_m) = 0$ is obeyed[...]
  zero-order Bessel's function[...]

- the light backscattered on[...]
  one mode into the other ca[...]
  onance by the Doppler eff[...]
  crystal movement in the c[...]
  nomenon, which induces a[...]
  sponding coupling strength,[...]
  ported in the case of vibrat[...]
  our model, it arises from the[...]
  factor $\exp(2ikx_c)$ in front[...]
  cients $\tilde{m}_{1,2}^c$ and $\int N_c\mathrm{d}x$ in e[...]

- the frequency non-reciproci[...]
  propagating modes due to t[...]
  ging effect – eq. (8) – has a[...]
  chanical dithering typically[...]
  the lock-in problem in the[...]
  laser gyroscopes [27].

The solid-state ring laser setup[...]
iment is sketched on Fig. 1. Th[...]
stabilizing coupling (4), a beat [...]
above a critical rotation speed, w[...]
ted on Fig. 2. It can be seen on this figure that the
difference between the ideal Sagnac line and the experi-
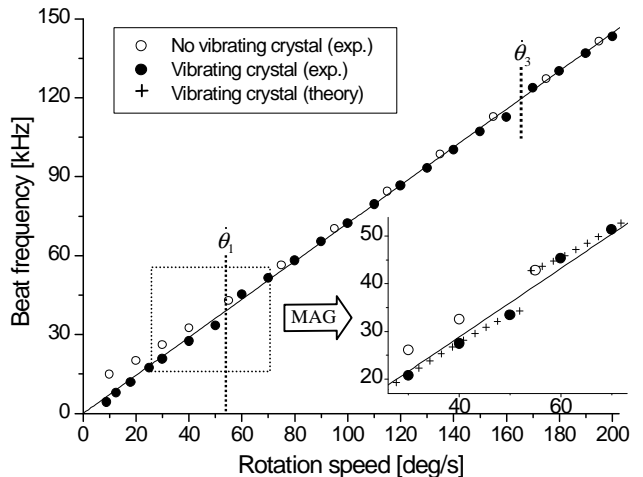mental beat frequency, which is a direct measurement of

Figure 2: Experimental beat frequency as a function of the
rotation speed. White and black circles refer respectively to
the situations where the crystal is at rest and where the crys-
tal is vibrating with a frequency $f_m \simeq 40$ kHz and an am-
plitude $x_m \simeq 0.74$ μm. The insert shows a magnification
around $\dot{\theta}_1$ – see eq. (10) –, together with theoretical predic-
tions resulting from numerical simulations with the following
measured [18] parameters : $\gamma = 15.34 \ 10^6$ s^{-1}, $\eta = 0.21$,
$|\tilde{m}_{1,2}^c| = 1.5 \ 10^4$ s^{-1}, $|\tilde{m}_{1,2}^m| = 8.5 \ 10^4$ s^{-1}, $\arg(\tilde{m}_1^c/\tilde{m}_2^c) =$
$\arg(\tilde{m}_1^m/\tilde{m}_2^m) = \pi/17$, $K = 10^7$ s^{-1}. Integration step is
0.1 μs, average values are computed between 8 and 10 ms.

the nonlinear interactions [14], is considerably reduced in
the zone ranging from 10 to 40 deg/s. Some nonlineari-
ties are observed around the discrete values $\dot{\theta} \simeq 55$ deg/s
and $\dot{\theta} \simeq 165$ deg/s, in agreement with our theoretical
model. As a matter of fact, analytical calculations start-
ing from equation (9) reveal the existence of disrupted
zones centered on discrete values of the rotation speed $\dot{\theta}_q$
obeying the following equation :

$$\frac{4A}{\lambda L}\dot{\theta}_q = qf_m \quad \text{where } q \text{ is an integer} , \quad (10)$$

the size of each disrupted zone being proportional to
$J_q(kx_m)$. With our experimental parameters, the first
critical velocity corresponds to $\dot{\theta}_1 = 55.5$ deg/s, the zones
observed on Fig. 2 corresponding to the cases $q = 1$ and
$q = 3$. The numerical simulations shown on the insert
of this figure are in good agreement with our analytical
and experimental data. Such a phenomenon of disrupted
zones has been reported previously in the case of gas ring
laser gyroscopes with mechanical dithering. It is some-
times designed as 'Shapiro steps' [27], in reference to an
equivalent effect in the field of Josephson junctions [28].

The dependence of the beat frequency on the ampli-
tude of the crystal movement is shown on Fig. 3, for
a fixed rotation speed (200 deg/s). This graph illus-
trates the good agreement between our numerical sim-
ulations and our experimental data. Moreover, this is an
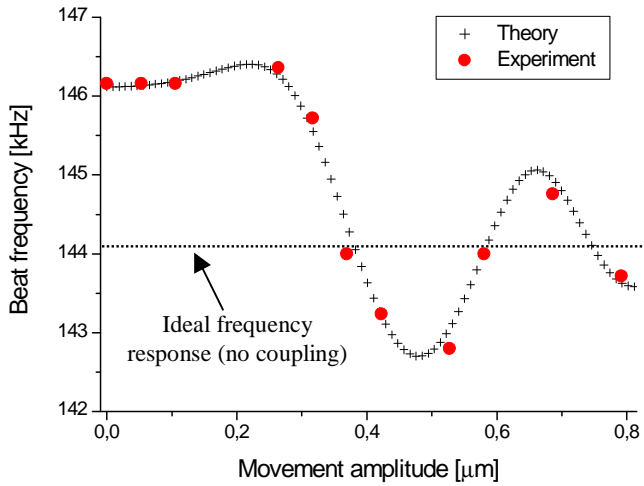experimental demonstration of the direct control of the

Figure 3: Beat frequency as a function of the amplitude of the crystal movement for $\dot\theta = 200$ deg/s. The theoretical values (crosses) come from the numerical integration of equation (9) with the same parameters as Fig. 2.

strength of nonlinear interactions in the solid-state ring laser. In particular, for some special amplitudes of the crystal movement, the influence of mode coupling vanishes, resulting in a beat frequency equal to the ideal Sagnac value.

This study suggests the use of a higher vibration frequency of the crystal, in order to increase the value of $\dot\theta_1$ as much as possible. When $f_m \gg |\Omega|/(2\pi)$, the strength of the nonlinear interactions is shown to be directly proportional to $J_0(kx_m)^2$, and the condition for rotation sensing reads :

$$2K\eta > \tilde{N} J_0(kx_m)^2 \ , \qquad (11)$$

where $\tilde{N} = \gamma\eta/(1 + \Omega^2 T_1^2)$ is the strength of nonlinear interactions [14], and $J_0(kx_m)^2$ is the attenuation factor due to the crystal vibration. The similar condition for rotation sensing in the case of a toroidal Bose-Einstein condensate, as derived in [13], is $V_0 > g$ (where V_0 is the asymmetry energy and g the mean (repulsive) interaction energy per particle in the s-wave state). It becomes, in the presence of Feshbach resonance induced by a magnetic field B as described in [15] :

$$V_0 > g \left(1 - \frac{\Delta}{B - B_0}\right) \ , \qquad (12)$$

where Δ and B_0 are characteristic parameters. In this equation, g represents the nonlinear interactions, and the attenuation factor is $1 - \Delta/(B - B_0)$. Condition (12) shows strong similarities with condition (11). In both cases, rotation sensing is favored if nonlinear interactions are lowered, the ideal case being $B = B_0 + \Delta$ for the toroidal Bose-Einstein condensed gas and $J_0(kx_m) = 0$ for the solid-state ring laser. The parameter for the control of nonlinear interactions is the magnetic field B in the first case and the movement amplitude x_m in the second case.

In conclusion, we have developed a concrete method for tuning and suppressing nonlinear interactions in the case of a solid-state ring laser, by vibrating the gain crystal along the cavity axis. Our theoretical model shows a very good agreement with the experiment. The observation of rotation sensing in the solid-state ring laser allows the direct measurement of the strength of nonlinear interactions, leading to the experimental demonstration of their fine tuning and even suppression. Furthermore, following the previous work of [14], we have underlined the analogy between our system and other ring-shaped macroscopic quantum configurations where nonlinear interactions could be tuned, for example a Bose-Einstein condensed gas with magnetically-induced Feshbach resonance. This illustrates the richness of such devices, both from applicative and fundamental perspectives.

---

* Electronic address: sylvain.schwartz@thalesgroup.com
[1] F. Aronowitz in *Laser Applications* (Academic, New York, 1971), p. 133.
[2] P. A. Khandokhin and Y. I. Khanin, J. Opt. Soc. Am. B **2**, 226 (1985).
[3] N. Kravtsov, E. Lariontsev, and A. Shelaev, Laser Phys. **3**, 21 (1993).
[4] F. Bloch, Phys. Rev. A **7**, 2187 (1973).
[5] A. Leggett, Rev. Mod. Phys. **71**, 318 (1999).
[6] O. Avenel, P. Hakonen and E. Varoquaux, Phys. Rev. Lett. **78**, 3602 (1997).
[7] K. Schwab, N. Bruckner and R.E. Packard, Nature **386**, 585 (1997).
[8] E. Mueller, P. Goldbart and Y. Lyanda-Geller, Phys. Rev. A **57**, R1505 (1998).
[9] M. Benakli *et al.*, Europhys. Lett. 46, 275 (1999).
[10] M. Cozzini, B. Jackson and S. Stringari, Phys. Rev. A **73**, 013603 (2006).
[11] S. Schwartz *et al.*, New J. Phys. **8**, 162 (2006).
[12] C. Ryu *et al.*, arXiv:0709.0012v1 [cond-mat.other].
[13] A. Leggett, Rev. Mod. Phys. **73**, 307 (2001).
[14] S. Schwartz *et al.*, Phys. Rev. Lett. **97**, 093902 (2006).
[15] S. Inouye *et al.*, Nature, **392**, 151 (1998).
[16] Ph. Courteille *et al.*, Phys. Rev. Lett. **81**, No. 1, 69 (1998).
[17] M. Fattori *et al.*, arXiv:0710.5131v1 [cond-mat.other].
[18] S. Schwartz *et al.*, Phys. Rev. A **76**, 023807 (2007).
[19] H. Danielmeyer and W. Nilsen, Appl. Phys. Lett. **16**, No. 3, 124 (1970).
[20] R. Spreeuw *et al.*, Phys. Rev. A **42**, No. 7, 4315 (1990).
[21] A. Siegman, *Lasers*, University Science Books, Mill Valley, California (1986).
[22] G. Sagnac, C.R. Acad. Sci. **157**, 708 (1913).

[23] H. R. Bilger and W. K. Stowell, Phys. Rev. A **16**, No. 1, 313 (1977).

[24] H. Sabert and R. Ulrich, Appl. Phys. Lett. **58**, No. 21, 2323 (1991).

[25] R. A. Patterson *et al.*, Proc. SPIE **487**, 78 (1984).

[26] M. Lai *et al.*, Opt. Lett. **17**, No. 21, 1535 (1992).

[27] W. Chow *et al.*, Rev. Mod. Phys. **57**, No. 1, 61 (1985).

[28] S. Shapiro, Phys. Rev. Lett. **11**, 80 (1963).